Frontiers of Materials Science

Electronic Supplementary Material

Direct fabrication of few-layer graphene via molten salt-assisted magnesiothermic reduction

Jie Liu[1,2], Binfeng Pan[1,2], Zhimin Zhang (✉)[1], and Xuchen Lu[1]

1 State Key Laboratory of Mesoscience and Engineering, Institute of Process Engineering, Chinese Academy of Sciences, Beijing 100190, China
2 School of Chemical Engineering, University of Chinese Academy of Sciences, Beijing 100049, China

E-mail: zmzhang@ipe.ac.cn

Experimental

Chemicals

K_2CO_3 (≥ 99.0 wt.%), $CaCO_3$ (≥ 99.0 wt.%), Mg powder (≥ 99.0 wt.%, 100–200 mesh), KCl (≥ 99.5 wt.%), and NaCl (≥ 99.5 wt.%) were all purchased from Sinopharm Chemical Reagent Co. and used as received without further purification.

Synthesis of few-layer turbostratic graphene

The resultant graphene was denoted as *K*-FLG, which means K_2CO_3-derived few-layer graphene (FLG). *K*-FLG was prepared via magnesiothermic reduction using K_2CO_3 as the precursor and eutectic chloride molten salt as the reaction media. In a typical experimental process, Mg (1.15 g), K_2CO_3 (2.76 g), NaCl (17.20 g), and KCl (21.90 g) powders were mixed evenly by grinding and then put into a 50 mL corundum crucible with a cover (the mass ratio of chlorides (i.e., NaCl–KCl) to reactants (i.e., Mg and K_2CO_3) is 10:1) to guarantee the full protection of the reaction process. Subsequently, the mixture was heated to 800 ℃ within 2 h and then maintained for 2 h. The entire heating process was conducted at ambient pressure and under ambient atmosphere. After cooling down naturally, the resulting sample was stirred in 180 mL HCl solution (2.0 $mol \cdot L^{-1}$) for 3 h at room temperature, followed by washing and filtrating with deionized water several times until a pH value of 7 was reached. Finally, absolute ethanol was used to rinse the isolated solid carbon product before vacuum-drying at 80 ℃ for more than 12 h. For comparison, two other samples were prepared by the same experimental procedure as that for preparing *K*-FLG, except for the choice of carbon source: (I) *Ca*-FLG, which means $CaCO_3$-derived FLG; (II) We only used Mg and $CaCO_3$ (without molten salt) to prepare this graphene sample (denoted as MCG).

Characterization

The morphology and the microstructure of the samples were characterized by field emission scanning electron microscopy (FESEM, JSM-7001F, Japan) operating at an accelerating voltage of 15 kV and transmission electron microscopy (TEM, JEM-2100F UHR, Japan) with an acceleration voltage of 200 kV, as well as high-resolution TEM (HRTEM, JEM-2100F UHR, Japan).

The crystal structures of the samples were investigated by X-ray diffraction (XRD, X'Pert PRO

MPD, Netherlands) with Cu Kα radiation (λ =1.5418 Å) performed at 40 kV and 40 mA, and the relative intensity was recorded in the scattering range of 5°–90° (2θ) within 5 min.

The Raman spectroscopy (Renishaw inVia, England) was used to characterize the molecular structure of the as-obtained graphene, which was operated at the excitation wavelength of 532 nm with a laser spot size of 1 mm on a quartz slide.

The surface chemical composition was analyzed by X-ray photoelectron spectroscopy (XPS, AXIS SUPRA+, Japan) with Al Kα (1486.6 eV) radiation as the excitation source. To correct the charging effects, all spectra were calibrated relative to the carbon C 1s peak positioned at 284.6 eV. Processing of XPS results was carried out using the Avantage program.

Nitrogen adsorption/desorption measurements were performed at the liquid nitrogen temperature (77 K) with a NOVA 3200e physisorption analyzer (Britain). Before measurements, samples were degassed at 200 ℃ under a high vacuum for at least 5 h. The specific surface area (SSA) was calculated according to the multi-point Brunauer–Emmett–Teller (BET) equation using the nitrogen adsorption data in the relative pressure (p/p_0) range of 0.05–0.99. The pore size distribution (PSD) was calculated from the adsorption data using the nonlocal density functional theory (NLDFT) equilibrium model method for cylinder/slit pores. The total pore volume was determined from the adsorbed amount at a relative pressure p/p_0 of 0.99.

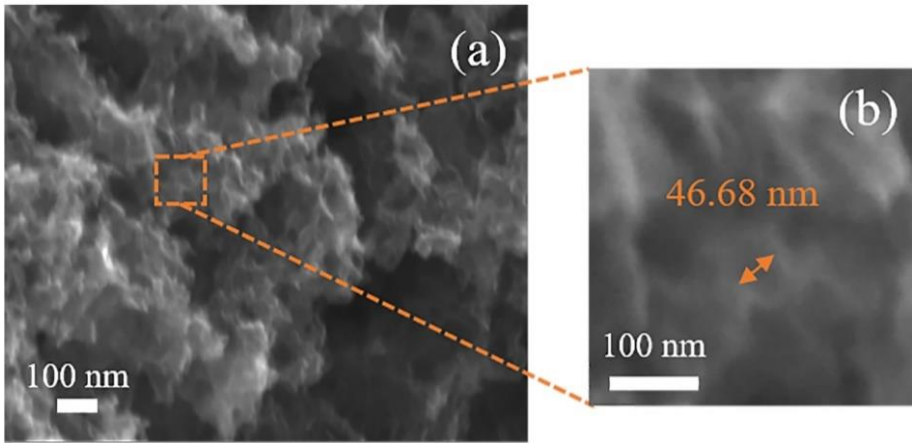

Fig. S1 (a) SEM image of *K*-FLG and **(b)** enlarged part marked in panel (a).

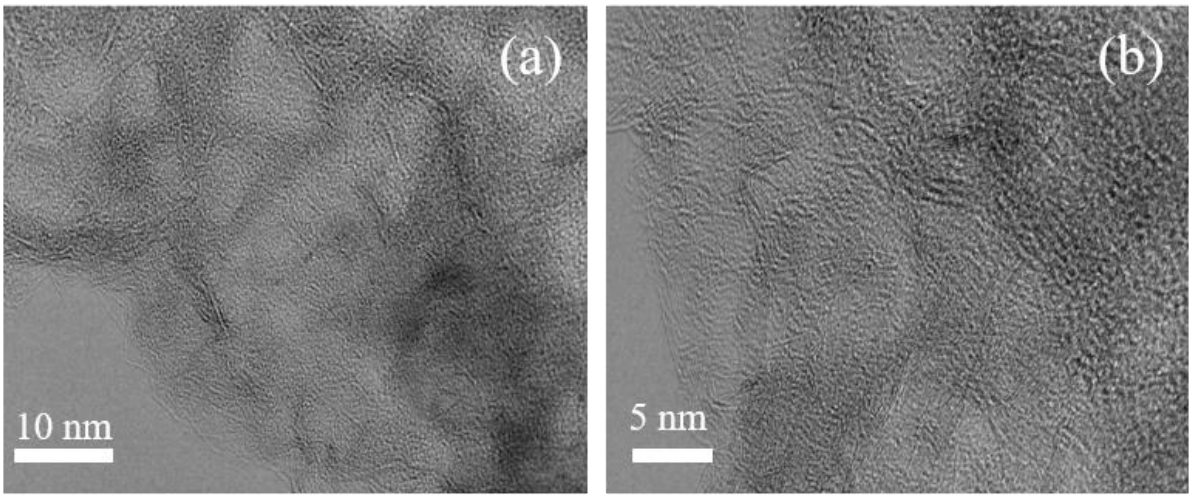

Fig. S2 HRTEM images of *Ca*-FLG with different resolutions: **(a)** scale bar measuring 10 nm; **(b)** scale bar measuring 5 nm.

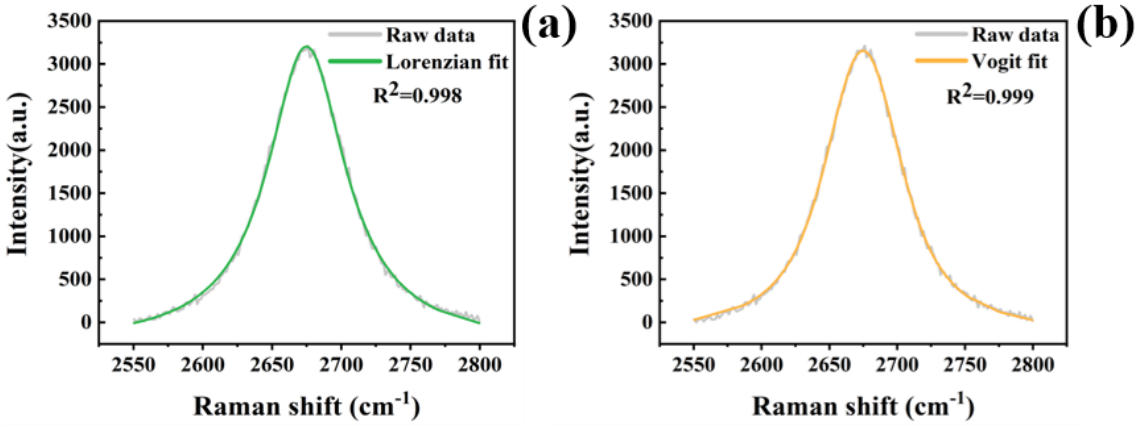

Fig. S3 Fitting of the 2D band of *K*-FLG: **(a)** Lorentzian function; **(b)** Voigt function.

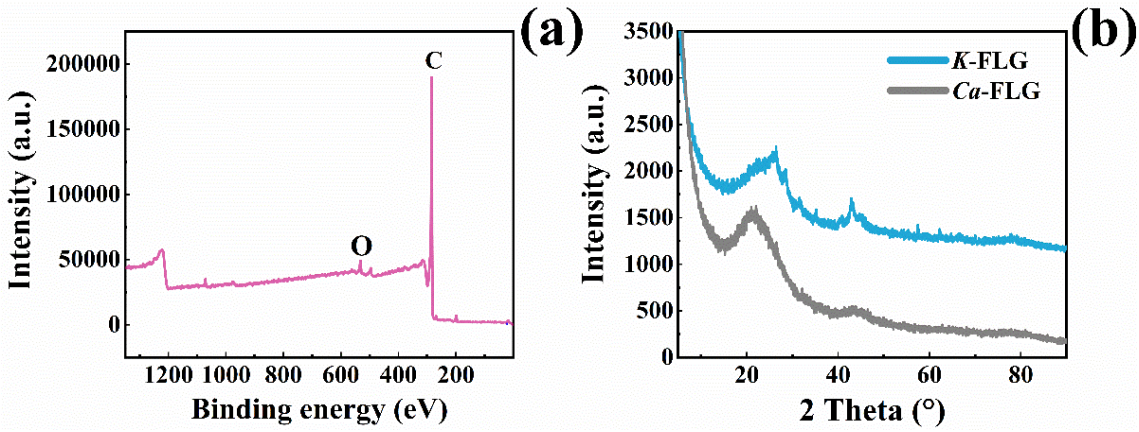

Fig. S4 (a) XPS full spectrum of *K*-FLG. **(b)** Comparison of XRD patterns between *K*-FLG and *Ca*-FLG.

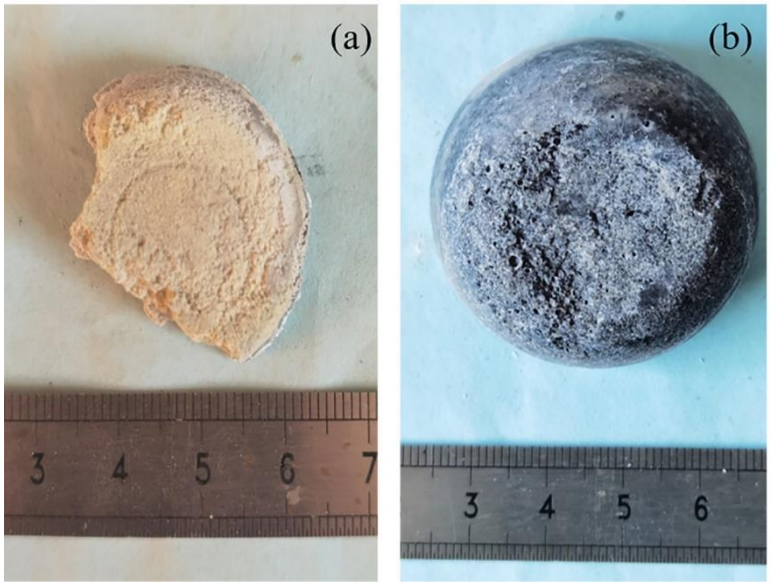

Fig. S5 Comparison of reaction systems between **(a)** Mg–K_2CO_3 and **(b)** Mg–K_2CO_3–NaCl–KCl heated at 650 °C for 2 h. Because both the K_2CO_3–NaCl–KCl ternary system and Mg powder started melting around 650 °C [1], the reaction kinetics are significantly improved. Thus, the evident black carbon or graphene-enveloped reaction system was observed. In stark contrast, no black carbon/graphene was observed in the reaction system of Mg–K_2CO_3, and the yellowish color might be attributed to the hydrolysis of K_2CO_3 at elevated temperatures.

Table S1 Graphitization of carbon by K_2CO_3 or K_2CO_3-containing molten salt at different temperatures

Carbon source	Molten salt	Preparation temperature/°C	Graphitization of products [a)]	Ref.
Peanut shell	Li_2CO_3–Na_2CO_3–K_2CO_3	850	No lattice fringe	[2]
Typha angustifolia	NaCl–K_2CO_3	800–850	No lattice fringe	[3]
Coal	Na_2CO_3–K_2CO_3	700	No lattice fringe	[4]
Coal tar pitch	K_2CO_3–KCl	600–800	No lattice fringe	[5]
Sodium glutamate	NaCl–Na_2CO_3	800	No lattice fringe	[6]
Kitchen waste	K_2CO_3	900	Obvious lattice fringe	[7]
Coconut shell	K_2CO_3	900	Obvious lattice fringe	[8]
Ginkgo leaf	KCl–K_2CO_3	900	Obvious lattice fringe	[9]
K_2CO_3	NaCl–KCl	800	Obvious lattice fringe	This work

a) The graphitization of products was characterized by the existence of lattice fringes using HRTEM analysis.

Table S2 Comparison of Raman results between *K*-FLG and products obtained via magnesiothermic reduction from various carbon sources

Carbon source	Preparation condition	I_D/I_G	I_{2D}/I_G	Position of 2D/cm^{-1}	FWHM of 2D/cm^{-1}	Ref.
$CaCO_3$	SHS [a)]	0.16–0.6	1–1.43	2665	41–54	[10] [d)]
$CaCO_3$	850 °C, 3 h	> 1	0.36	2645	–	[11]
$CaCO_3$	SHS	0.81	0.32	2678	–	[12] [b)]
$MgCO_3$	SHS	0.54	0.49	2679	–	[12] [b)]
$CaCO_3$	High pressure, 670–760 °C, 1 h	1.0–1.3	–	2680	–	[13] [b)]
Eggshell and crab shell	700 °C, 5 h, gas–solid reaction	0.56	–	2684	–	[14] [c)]
CO_2	600–1000 °C	1.36–1.58	–	–	–	[15] [c)]
CO_2	700 °C, 0.5 h	0.98	0.61–0.70	2678	–	[16] [b,e)]
CO_2	SHS	–	–	2672	weak	[17] [b)]
CO_2	SHS	–	1.78	2700	30.5	[18] [c)]
CaC_2O_4/MgC_2O_4	SHS	0.33	3.30	–	–	[19]
$H_2C_2O_4$	High pressure or vacuum	> 1	–	2626	weak	[20]
C_6H_4COOK	800 °C, 2 h	2.03–2.21	–	–	–	[21] [c)]
K_2CO_3	800 °C, 2 h	0.82	1.95	2675	70	This work

a): SHS is the abbreviation of self-propagating high-temperature synthesis.
b), c), d): In view of effects of the laser wavelength on results, the wavelength used in above experiments is provided, representing 532, 514, and 633 nm, respectively.
e) Mg powder and carbon source were separated in the reactor, and those two were mixed in the rest of the experiments.

Table S3 Comparison of XPS atomic C/O ratios and SSAs between *K*-FLG and products obtained via magnesiothermic reduction from various carbon sources

Carbon source	Preparation condition	XPS atomic C/O ratio	SSA/($m^2 \cdot g^{-1}$)	Ref.
$CaCO_3$	High pressure, 670–760 °C, 1 h	10	744	[13]
$CaCO_3$	SHS	16–25	–	[12]
$MgCO_3$	SHS	16–25	–	[12]
Eggshell and crab shell	700 °C, 5 h, gas–solid reaction	17	551	[14]
CO_2	700 °C, 0.5 h	18	52	[16]
CO_2	SHS	82	709	[17]
CO_2	SHS	25	–	[18]
Coal tar pitch	K_2CO_3 as catalyst for graphitization	44.6–61.5	1490–2113	[22]
Raisin	Laser-assisted treatment	19	32	[23]
GO hydrogel	HI–HAc reduction	2.6–7.1	290	[24]
Coconut shell	K_2CO_3 as activator, 900 °C	12	1506	[8]
K_2CO_3	800 °C, 2 h	32	748	This work

References

[1] Yaokawa J, Oikawa K, Anzai K. Thermodynamic assessment of the KCl–K_2CO_3–NaCl–Na_2CO_3 system. Calphad - Computer Coupling of Phase Diagrams and Thermochemistry, 2007, 31(2): 155–163

[2] Yin H, Lu B, Xu Y, et al. Harvesting capacitive carbon by carbonization of waste biomass in molten salts. Environmental Science & Technology, 2014, 48(14): 8101–8108

[3] Wang S, Mei Y, Shao Z, et al. Biomass hierarchical porous carbonized typha angustifolia prepared by green pore-making technology for energy storage. ACS Omega, 2023, 8(1): 1353–1361

[4] Dong P, Wu X, Lv Y, et al. Coal-based 2D ultrathin N-doped hierarchical porous carbon nanosheets induced by dual-salt system of Na_2CO_3–K_2CO_3 for high-performance supercapacitors. Energy & Fuels, 2024, 38(14): 13344–13354

[5] Ren P, Wu D, Wang T, et al. K_2CO_3–KCl acts as a molten salt flame retardant to prepare N and O doped honeycomb-like carbon in air for supercapacitors. Journal of Power Sources, 2022, 532: 231072

[6] Qian W, Zhu J, Zhang Y, et al. Condiment-derived 3D architecture porous carbon for electrochemical supercapacitors. Small, 2015, 11(37): 4959–4969

[7] Du X, Lin Z, Zhang Y, et al. Microstructural tailoring of porous few-layer graphene-like biochar from kitchen waste hydrolysis residue in molten carbonate medium: Structural evolution and conductive additive-free supercapacitor application. Science of the Total Environment, 2023, 871: 162045

[8] Xia J, Zhang N, Chong S, et al. Three-dimensional porous graphene-like sheets synthesized from biocarbon via low-temperature graphitization for a supercapacitor. Green Chemistry, 2018, 20(3): 694–700

[9] Tian H, Fang Q, Cheng R, et al. Molten salt template-assisted synthesis of N, S-codoped hierarchically porous carbon nanosheets for efficient energy storage. Colloids and Surfaces A: Physicochemical and Engineering Aspects, 2021, 614: 126172

[10] Yin H, Chen P, Xu C, et al. Shock-wave synthesis of multilayer graphene and nitrogen-doped graphene materials from carbonate. Carbon, 2015, 94: 928–935

[11] Zhao J, Guo Y, Li Z, et al. An approach for synthesizing graphene with calcium carbonate and magnesium. Carbon, 2012, 50(13): 4939–4944

[12] Wang L, Wei B, Dong P, et al. Large-scale synthesis of few-layer graphene from magnesium and different carbon sources and its application in dye-sensitized solar cells. Materials & Design, 2016, 92: 462–470

[13] Han T, Sun B, Li Q, et al. Scalable synthesis and electrochemical performance of mesoporous graphene from calcium carbonate by magnesiothermic reaction. Progress in Natural Science: Materials International, 2022, 32(3): 289–295

[14] Tang H, Gao P, Liu X, et al. Bio-derived calcite as a sustainable source for graphene as high-performance electrode material for energy storage. Journal of Materials Chemistry A, 2014, 2(38): 15734–15739

[15] Zhang H, Zhang X, Sun X, et al. Shape-controlled synthesis of nanocarbons through direct conversion of carbon dioxide. Scientific Reports, 2013, 3: 3534

[16] Li X, Wang X, Hu X, et al. Direct conversion of CO_2 to graphene via vapor–liquid reaction for magnesium matrix composites with structural and functional properties. Journal of Magnesium and Alloys, 2023, 11(4): 1206–1212

[17] Li C, Zhang X, Wang K, et al. Scalable self-propagating high-temperature synthesis of graphene for supercapacitors with superior power density and cyclic stability. Advanced Materials, 2017, 29(7): 1604690

[18] Kim T H, Merritt C R, Ducati C, et al. Bulk synthesis of graphene-like materials possessing turbostratic graphite and graphene nanodomains via combustion of magnesium in carbon dioxide. Carbon, 2019, 149: 582–586

[19] Huczko A, Kurcz M, Dabrowska A, et al. Synthesis of 3-D graphene via combustion synthesis of magnesium and calcium/magnesium oxalates. ECS Journal of Solid State Science and Technology, 2017, 6(6): M3090–

M3096

[20] Dyjak S, Kicinski W, Norek M, et al. Hierarchical, nanoporous graphenic carbon materials through an instant, self-sustaining magnesiothermic reduction. Carbon, 2016, 96: 937–946

[21] Zhang Z J, Chen X Y, Xie D H, et al. Temperature-dependent structure and electrochemical performance of highly nanoporous carbon from potassium biphthalate and magnesium powder via a template carbonization process. Journal of Materials Chemistry A, 2014, 2(25): 9675–9683

[22] Pham V H, Wang C, Gao Y, et al. Synthesis of microscopic 3D graphene for high-performance supercapacitors with ultra-high areal capacitance. Small Methods, 2024, 8(9): 2301426

[23] Athanasiou M, Samartzis N, Sygellou L, et al. High-quality laser-assisted biomass-based turbostratic graphene for high-performance supercapacitors. Carbon, 2021, 172: 750–761

[24] Xiong Z, Liao C, Han W, et al. Mechanically tough large-area hierarchical porous graphene films for high-performance flexible supercapacitor applications. Advanced Materials, 2015, 27(30): 4469–4475